Supporting information for: Isotope effect of mercury diffusion in air

Paul G. Koster van Groos[1†], *Bradley K. Esser*[2], *Ross W. Williams*[2], *James R. Hunt*[1]

[1]Department of Civil and Environmental Engineering, University of California at Berkeley, Berkeley, California, 94720-1710 USA

[2]Chemical Sciences Division, Lawrence Livermore National Laboratory, P.O. Box 808, L-231, Livermore, California, 94551 USA

Email: pkostervangroos@gmail.com

14 pages (including cover page)

Description of:
- **Instrument mass bias corrections,**
- **Determining delta values, and**
- **Measurement of standards**

4 tables

6 figures

Instrumental mass bias corrections

One drawback of ICP-MS instruments is that measured isotope values are altered by the instrument itself. This instrumental mass bias effect can be as large as several percent. In the mercury system, several approaches to correct for this effect have been used, including simple standard-sample bracketing[1] and mercury double spike addition,[2] but most commonly spiking with thallium.[3–5] This later method uses observed variations in the $^{205}Tl/^{203}Tl$ ratio to correct instrumental variations in mercury isotope ratios and this is the approach used in this work. Most researchers to date have applied an exponential fractionation law to correct for instrumental mass bias.

This work approaches instrumental mass bias correction slightly differently by using an empirical approach as outlined by Marechal et al.[6] and described for the mercury system by Meija et al.[7] The empirical approach was determined to be the most appropriate for avoiding biases. Additionally, an empirical approach may compensate for unaccounted factors. The empirical approach is to observe the log-linear behavior of mercury and thallium isotope ratios following the general equation:

$$\ln\left(\frac{^{x}Hg}{^{198}Hg}\right) = a + b * \ln\left(\frac{^{205}Tl}{^{203}Tl}\right) \qquad 1,$$

Where *a* and *b* are least squares estimates determined for each analytical run. Figure SI-S1 illustrates this approach using the NIST 3133 standard. Without correction, the measured $^{202}Hg/^{198}Hg$ ratios for NIST 3133 shown in the figure vary by approximately 4‰. The estimated 2SD of individual NIST 3133 measurements from the estimated linear behavior is 0.35‰. During analytical sessions, deviations from linear behavior for NIST 3133 were used to estimate in-run uncertainty.

The instrumental mass bias is a function of the ion composition generated in the plasma and traveling through the mass spectrometer. It is important that standards and samples are matched by concentration and solution matrix. In this work, solution matrices were matched as much as possible, and concentrations were matched within 15%.

Determining delta values

There is currently no mercury standard sufficiently well characterized to allow variations in mercury isotope compositions to be reported with absolute ratios. Instead, isotope ratios are determined relative to a commonly available standard. As suggested by Blum and Bergquist,[8] this work uses the NIST 3133 SRM as the reference standard and relative isotope ratios are reported as delta (δ)-values. Formally, δ-values used in this work are for ratios relative to ^{198}Hg and defined as follows:

$$\delta^{x}Hg(‰) = 1000 * \left[\left(\frac{^{x}Hg}{^{198}Hg} \right)_{Sample} \Big/ \left(\frac{^{x}Hg}{^{198}Hg} \right)_{NIST3133} - 1 \right] \quad (2)$$

Practically, when $(^{xxx}Hg/^{198}Hg)_{sample} \approx (^{xxx}Hg/^{198}Hg)_{NIST3133}$, as is the case with samples near natural abundances, delta values can be estimated as follows:

$$\delta^{x}Hg(‰) \approx 1000 * \left[\ln\left(\frac{^{x}Hg}{^{198}Hg} \right)_{Sample} - \ln\left(\frac{^{x}Hg}{^{198}Hg} \right)_{NIST3133} \right] \quad (3)$$

The errors introduced with this simplification are significantly smaller than errors associated with measurements. δ values in this work were estimated using equation 3, where the value for NIST 3133 at the same ^{205}Tl/^{203}Tl value is estimated with the linear behavior described above. This is illustrated in Figure SI-S1 for a sample from experiment 2. Because the mass bias and the

equivalent NIST 3133 value is estimated at the same $^{205}Tl/^{203}Tl$ ratio as the sample, there is no additional need for standard-sample bracketing. Care should be taken to ensure than the range of $^{205}Tl/^{203}Tl$ measured at the same time as NIST 3133 covers the range for the samples to be measured.

Measurements of standards

It is important to repeatedly measure standards other than the reference standard (NIST 3133) to assess the long-term reproducibility of measurements and to allow inter-laboratory comparisons. Figure SI-S2 shows repeated measurements of a mercury standard produced from the Almaden Mine in Spain, UM-Almaden, kindly provided by Professor Joel Blum of the University of Michigan. The errors shown for individual sample points are the greater of: i) two times the estimated in-run standard deviation (2SD) based on NIST 3133 as described above, or ii) two times the estimated standard error (2SE) of sample replicates during the analytical run. The UM-Almaden standard has been shared among several laboratories and Table SI-S1 shows reported values and errors found in the literature. The long-term $\delta^{202}Hg$ value for the UM-Almaden reported here, -0.69±0.27‰, is more negative but not significantly different than other reported values.

Figure SI-S3 shows the long-term reproducibility of a secondary in-house mercury standard available during this work. The reproducibility of this standard was similar to that of UM-Almaden. There is an interesting outlier among the secondary standard measurements, indicated with an asterisk. This was an older standard kept in a plastic centrifuge tube that had lost approximately 30% of its mercury mass. This loss of mercury was accompanied by significant isotope fractionation on the order of 1‰ in $\delta^{202}Hg$.

Table SI-S1. Literature δ^{202}Hg values for UM-Almaden standard. Errors are 2SD

Reference	δ^{202}Hg (‰) (2SD)
This work	-0.69±0.27
8*	-0.54±0.08
8*	-0.58±0.15
9*	-0.61±0.12
9*	-0.51±0.17
1*	-0.61±0.24
1*	-0.58±0.09
10	-0.57±0.07
11	-0.48±0.16
12	-0.48±0.11
2	-0.58±0.08

* Multiple δ^{202}Hg values for the UM-Almaden standard are reported in these publications reflecting different methodologies such as sample matrix, introduction method, and concentration

Table SI-S2. Isotope ratios and masses of mercury in standards and samples. For the UM-Almaden and LLNL secondary standards, n represents the total number of analytical sessions using the average isotope values during each session. For the recovered standards, n represents the number of standards processed and measured and the isotope values are the mean value of the session. For the samples, n represents the number of measurements of sample. The asterisk(*) indicates a sample that was not used for isotope analyses.

		Recovery during sample preparation	n	δ^{202}Hg	δ^{201}Hg	δ^{200}Hg	δ^{199}Hg			
UM-Almaden standard			11	-0.69±0.27	-0.57±0.23	-0.34±0.15	-0.20±0.20			
LLNL secondary standard			13	-0.96±0.14	-0.74±0.12	-0.47±0.10	-0.21±0.09			
Experiment 1 NIST 3133 Recovered		0.48	3	1.07±0.36	0.64±0.34	0.46±0.22	0.05±0.19			
Experiment 2 & 3 NIST 3133 Recovered		0.96	3	-0.12±0.35	-0.04±0.30	0.00±0.23	0.05±0.22			
Experiment 2 & 3 UM-Almaden Recovered		0.94	2	-0.71±0.35	-0.52±0.30	-0.31±0.23	-0.15±0.22			
	Sample							Time	Fraction remaining	Mass remaining
Experiment 1	1	0.50	3	0.02±0.36	0.01±0.34	0.01±0.22	-0.05±0.19	55	0.89	1327±92
	2	0.51	3	0.31±0.36	0.30±0.34	0.22±0.22	0.18±0.19	115	0.8	1201±60
	3	0.58	3	0.57±0.36	0.49±0.34	0.33±0.22	0.18±0.19	248	0.65	970±66
	4	0.57	3	0.57±0.36	0.52±0.34	0.34±0.22	0.24±0.19	361	0.55	821±41
	5	0.57	3	0.91±0.36	0.75±0.34	0.50±0.22	0.29±0.19	477	0.45	680±34
	6	0.36	3	2.24±0.36	1.74±0.34	1.18±0.22	0.59±0.19	1099	0.18	274±56
	7	0.36	3	2.28±0.36	1.80±0.34	1.17±0.22	0.61±0.19	1242	0.15	228±20
	8	0.45	3	3.02±0.36	2.34±0.34	1.57±0.22	0.79±0.19	1398	0.11	163±63
	9*	0.63	3	2.20±0.36	1.40±0.34	1.00±0.22	0.22±0.19	1547	0.076	114±37
	10	0.48	3	0.46±0.36	0.48±0.34	0.30±0.22	0.17±0.19	0	0.9	1346±155
Experiment 2	1	0.99	3	0.12±0.35	0.15±0.30	0.06±0.23	0.03±0.22	165	0.74	1107±55
	2	0.97	3	0.85±0.35	0.59±0.30	0.34±0.23	0.17±0.22	554	0.41	618±31
	3	0.97	3	2.14±0.35	1.55±0.30	0.99±0.23	0.51±0.22	1216	0.16	234±12
	4	0.87	3	2.66±0.35	1.94±0.30	1.33±0.23	0.69±0.22	1492	0.11	160±14
	5	0.89	3	2.97±0.35	2.26±0.30	1.49±0.23	0.86±0.22	1662	0.08	127±6
	6	0.92	3	0.10±0.35	0.02±0.30	0.01±0.23	0.02±0.22	1	0.92	1377±209
Experiment 3	1	0.95	3	-0.01±0.35	0.00±0.30	-0.07±0.23	-0.08±0.22	164	0.77	1158±58
	2	1.03	3	0.68±0.35	0.48±0.30	0.34±0.23	0.11±0.22	553	0.51	761±38
	3	0.93	3	1.64±0.35	1.30±0.30	0.80±0.23	0.48±0.22	1216	0.26	395±20
	4	0.95	3	2.01±0.35	1.48±0.30	0.99±0.23	0.53±0.22	1491	0.2	295±15
	5	0.92	3	0.10±0.35	0.02±0.30	0.01±0.23	0.02±0.22	1	0.92	1377±209

Table SI-S3. Literature values for bulk gas-phase Hg^0 diffusion coefficients.

Gas Composition	Reference	Temperature (°C)	Diffusion Coefficient (cm^2/s)
Hg-Air	This experiment	23	0.131±0.010
Hg-Air	[13]	25	0.1423±0.0003
Hg-Air	[14]	23	0.138±0.008*
Hg-N_2	[15]	19-25	0.138±0.019
Hg-N_2	[16]	28	0.13±0.01
Hg-N_2	[17]	156-317	0.273-0.482
Hg-N_2	[17]	23	0.144*
Hg-N_2	[14]	23	0.140±0.007*

* The diffusion coefficients are estimated at temperature given the relationships provided

Table SI-S4. Observed isotope fractionation factors in the air diffusion experiments and associated relative diffusion rates.

Experiment	α_{199}	H_{198}/H_{199}	D_{198}/D_{199}
1	1.00034±0.00008	1.000011	1.00033±0.00008
2	1.00035±0.00010	1.000011	1.00034±0.00010
3	1.00040±0.00017	1.000011	1.00039±0.00017
Weighted Average	1.00035±0.00006	1.000011	1.00034±0.00006

Experiment	α_{200}	H_{198}/H_{200}	D_{198}/D_{200}
1	1.00063±0.00011	1.000023	1.00062±0.00011
2	1.00064±0.00010	1.000023	1.00063±0.00010
3	1.00070±0.00018	1.000023	1.00069±0.00018
Weighted Average	1.00064±0.00007	1.000023	1.00063±0.00007

Experiment	α_{201}	H_{198}/H_{201}	D_{198}/D_{201}
1	1.00095±0.00014	1.000034	1.00093±0.00014
2	1.00094±0.00014	1.000034	1.00092±0.00014
3	1.00105±0.00023	1.000034	1.00103±0.00023
Weighted Average	1.00096±0.00011	1.000034	1.00094±0.00009

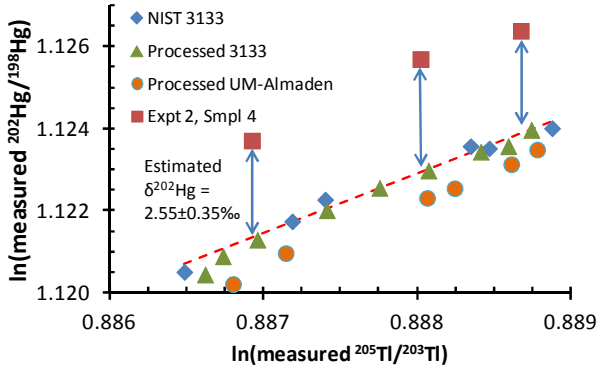

Figure SI-S1. Log plot of measured $^{202}Hg/^{198}Hg$ vs measured $^{205}Tl/^{203}Tl$ for NIST 3133, two processed standards, and one sample illustrating the mass bias correction approach. The dotted line indicates the best estimate of NIST 3133 upon instrumental fractionation of Hg and Tl.

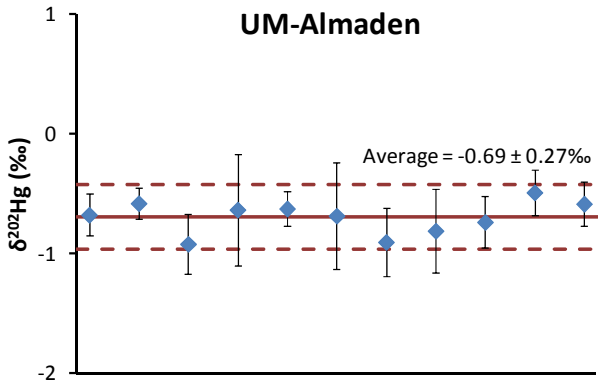

Figure SI-S2. Measured $\delta^{202}Hg$ values for the UM-Almaden mercury standard.

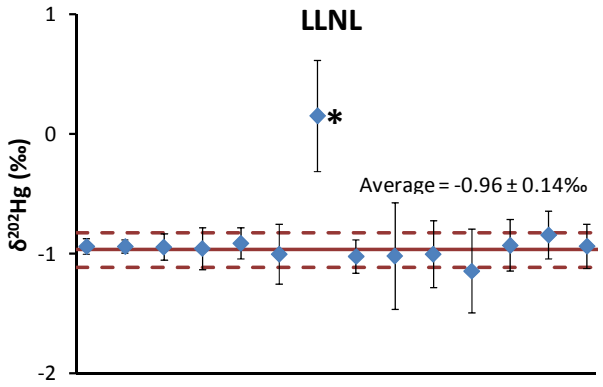

Figure SI-S3. Measured δ^{202}Hg values for the In-House LLNL mercury standard. The asterisk indicates an outlier discussed further in the text

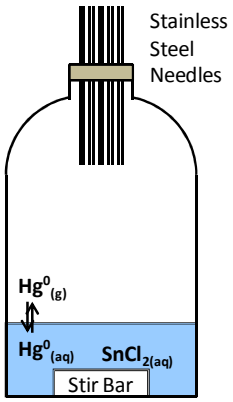

Figure SI-S4. Diagram of diffusion reactors used for determining mercury diffusion coefficients and isotope fractionation factors.

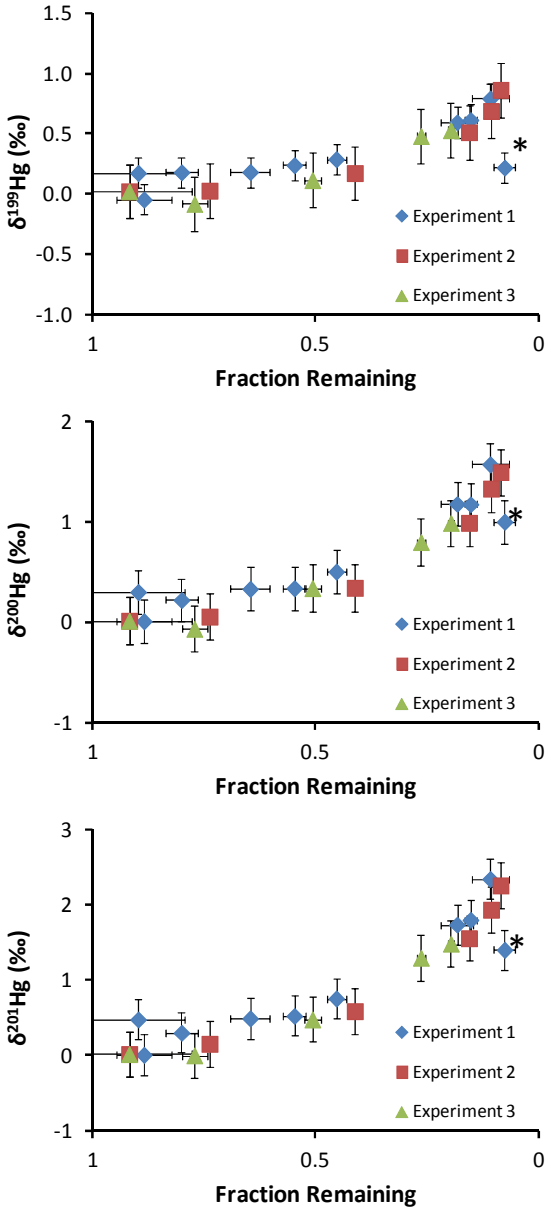

Figure SI-S5. δ^{199}Hg, δ^{200}Hg, and δ^{201}Hg of mercury remaining in the diffusion reactors. The asterisk (*) identifies an outlier not used during analysis. Experiments 1 and 2 used 2.54 cm needles while experiment 3 used 3.81 cm needles.

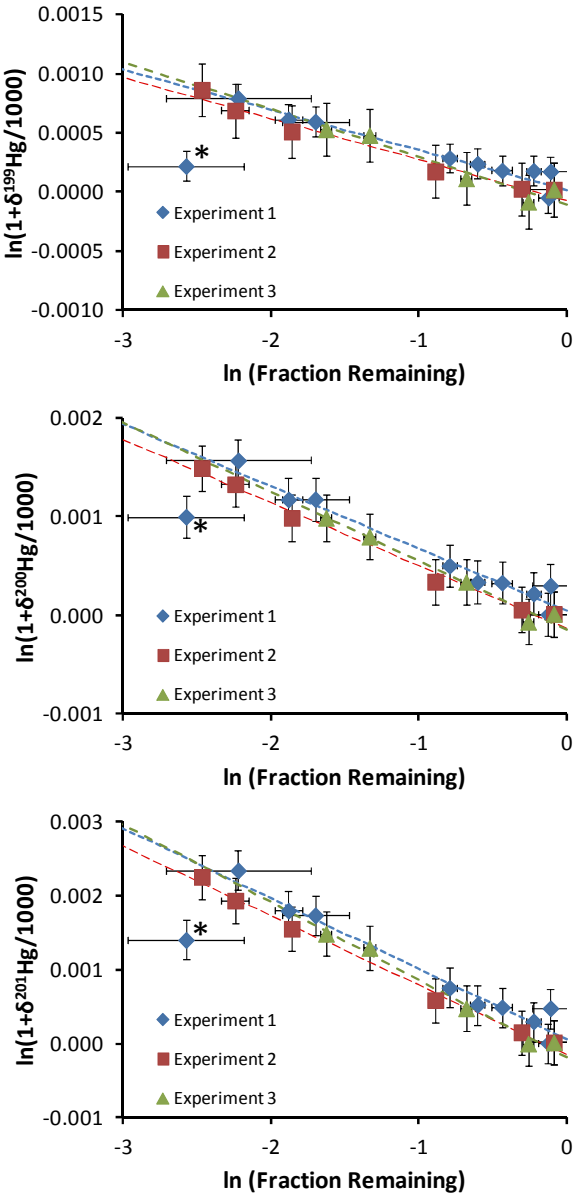

Figure SI-S6. Linearized isotope fractionation of δ^{199}Hg, δ^{200}Hg, and δ^{201}Hg. The asterisk (*) identifies an outlier not used in analysis.

REFERENCES

(1) Stetson, S. J.; Gray, J. E.; Wanty, R. B.; Macalady, D. L. Isotopic variability of mercury in ore, mine-waste calcine, and leachates of mine-waste calcine from areas mined for mercury. *Environ. Sci. Technol.* **2009**, *43*, 7331–7336.

(2) Mead, C.; Johnson, T. M. Hg stable isotope analysis by the double-spike method. *Anal. Bioanal. Chem.* **2010**, *397*, 1529–38.

(3) Hintelmann, H.; Lu, S. High precision isotope ratio measurements of mercury isotopes in cinnabar ores using multi-collector inductively coupled plasma mass spectrometry. *Analyst* **2003**, *128*, 635–639.

(4) Smith, C. N.; Kesler, S. E.; Klaue, B.; Blum, J. D. Mercury isotope fractionation in fossil hydrothermal systems. *Geology* **2005**, *33*, 825–828.

(5) Evans, R. D.; Hintelmann, H.; Dillon, P. J. Measurement of high precision isotope ratios for mercury from coals using transient signals. *J. Anal. At. Spectrom.* **2001**, *16*, 1064–1069.

(6) Marechal, C. N.; Telouk, P.; Albarede, F. Precise analysis of copper and zinc isotopic compositions by plasma-source mass spectrometry. *Chem. Geol.* **1999**, *156*, 251–273.

(7) Meija, J.; Yang, L.; Sturgeon, R. E.; Mester, Z. Certification of natural isotopic abundance inorganic mercury reference material NIMS-1 for absolute isotopic composition and atomic weight. *J. Anal. At. Spectrom.* **2010**, *25*, 384–389.

(8) Blum, J. D.; Bergquist, B. A. Reporting of variations in the natural isotopic composition of mercury. *Anal. Bioanal. Chem.* **2007**, *388*, 353–9.

(9) Epov, V. N.; Rodriguez-Gonzalez, P.; Sonke, J. E.; Tessier, E.; Amouroux, D.; Bourgoin, L. M.; Donard, O. F. X. Simultaneous determination of species-specific isotopic composition of Hg by gas chromatography coupled to multicollector ICPMS. *Anal. Chem.* **2008**, *80*, 3530–8.

(10) Zheng, W.; Hintelmann, H. Nuclear field shift effect in isotope fractionation of mercury during abiotic reduction in the absence of light. *J. Phys. Chem. A* **2010**, *114*, 4238–45.

(11) Sonke, J. E.; Schäfer, J.; Chmeleff, J.; Audry, S.; Blanc, G.; Dupré, B. Sedimentary mercury stable isotope records of atmospheric and riverine pollution from two major European heavy metal refineries. *Chem. Geol.* **2010**, *279*, 90–100.

(12) Wiederhold, J. G.; Cramer, C. J.; Daniel, K.; Infante, I.; Bourdon, B.; Kretzschmar, R. Equilibrium mercury isotope fractionation between dissolved Hg(II) species and thiol-bound Hg. *Environ. Sci. Technol.* **2010**, *44*, 4191–4197.

(13) Lugg, G. A. Diffusion coefficients of some organic and other vapors in air. *Anal. Chem.* **1968**, *40*, 1072–1077.

(14) Massman, W. J. Molecular diffusivities of Hg vapor in air, O2 and N2 near STP and the kinematic viscosity and thermal diffusivity of air near STP. *Atmos. Environ.* **1999**, *33*, 453–457.

(15) Spier, J. L. The determination of the coefficient of diffusion of mercury vapour and cadmium vapour in nitrogen. *Physica* **1940**, *7*, 381–384.

(16) Nakayama, K. An accurate measurement of the mercury vapor drag effect in the pressure region of transition flow. *Jpn. J. Appl. Phys.* **1968**, *7*, 1114–1119.

(17) Gardner, P. J.; Pang, P.; Preston, S. R. Binary gaseous diffusion coefficients of mercury and of zinc in hydrogen, helium, argon, nitrogen, and carbon dioxide. *J. Chem. Eng. Data* **1991**, *36*, 265–268.